Fermat's principle and ray tracing in anisotropic layered media

Joe Wong

ABSTRACT

I consider the path followed by a seismic signal travelling through velocity models consisting of horizontal layers, and describe a ray-bending method based on Fermat's principle, which states that the raypath between the source and receiver must be the one with the least travel time. The intersection points of the least-time raypath with the layer boundaries can be found by a direct-search nonlinear optimization routine. TTI velocity anisotropy can be included in one or more of the layers. An efficient and accurate procedure for producing raypaths and first-arrival times through these layers can be formulated using the Byun/Kumar approximation for TTI group velocities. The method was implemented in MATLAB code, and I present examples of least-time raypaths and travel times for sources and receivers embedded in isotropic and anisotropic layers.

INTRODUCTION

Kumar et al. (2004) and Casasanta et al. (2008) described a two-point ray-bending scheme on a VTI velocity field that is both efficient and accurate. VTI velocity anisotropy has a vertical axis of symmetry, with group velocities dependent on dip angle but invariant with azimuth angles about this axis. They formulated their algorithm using an approximation to the P-wave group velocity published by Byun et al. (1989):

$$V_p^{-2}(\emptyset) = a_0 + a_1 \cos^2\emptyset - a_2 \cos^4\emptyset \ , \tag{1}$$

$$a_0 = V_h^{-2} \ , \tag{2}$$

$$a_1 = 4V_{45}^{-2} - 3V_h^{-2} - V_v^{-2} \ , \tag{3}$$

$$a_2 = 4V_{45}^{-2} - 2V_h^{-2} - 2V_v^{-2} \ , \tag{4}$$

where V_v, V_h, and V_{45} are the group velocities in the vertical (∅=0°), horizontal (∅=90°), and 45° dip angle directions. For the isotropic case, a_1 and a_1 are identically zero.

Kumar et al. (2004) and Casasanta et al. (2008) compared quasi-P (qP) group velocities, raypaths, and travel times using Equations 1 to 4 with results from the exact treatment of VTI and from the Thomsen approximations (Thomsen, 1986). They showed that the Byun formulation gave better results than the Thomsen approximations in that they were closer to results derived from the exact treatment of VTI.

The horizontal and vertical velocities V_h and V_v are parameters whose values are intuitive and easily understood. The velocity V_{45} is less well understood, but nevertheless must be estimated and assigned a value. Following Kumar et al. (2004), I use Equations 16(a) and 22(a) from Thomsen (1986) to calculate a value for V_{45}, assuming values for the Thomsen parameters ε and δ, and then estimating the phase velocity angle θ corresponding to ∅ = 45°.

If we maintain VTI anisotropy, but tilt the symmetry axis by an angle φ in the x-z plane, we have tilted transverse isotropy (TTI). Equation 1 still applies, but the angle $\emptyset$ changes to $(\emptyset + \varphi)$,

$$V_p^{-2}(\emptyset) = a_0 + a_1 \cos^2(\emptyset + \varphi) - a_2 \cos^4(\emptyset + \varphi) \ . \quad (5)$$

Expanding $\cos(\emptyset + \varphi)$, we have:

$$\cos(\emptyset + \varphi) = \cos(\emptyset)\cos(\varphi) - \sin(\emptyset)\sin(\varphi) \ . \quad (6)$$

Because the depth coordinate is defined to be positive downwards, angles φ and $\emptyset$ are referenced to a down-pointing vertical vector. Positive φ rotates the VTI axis of symmetry counter-clockwise.

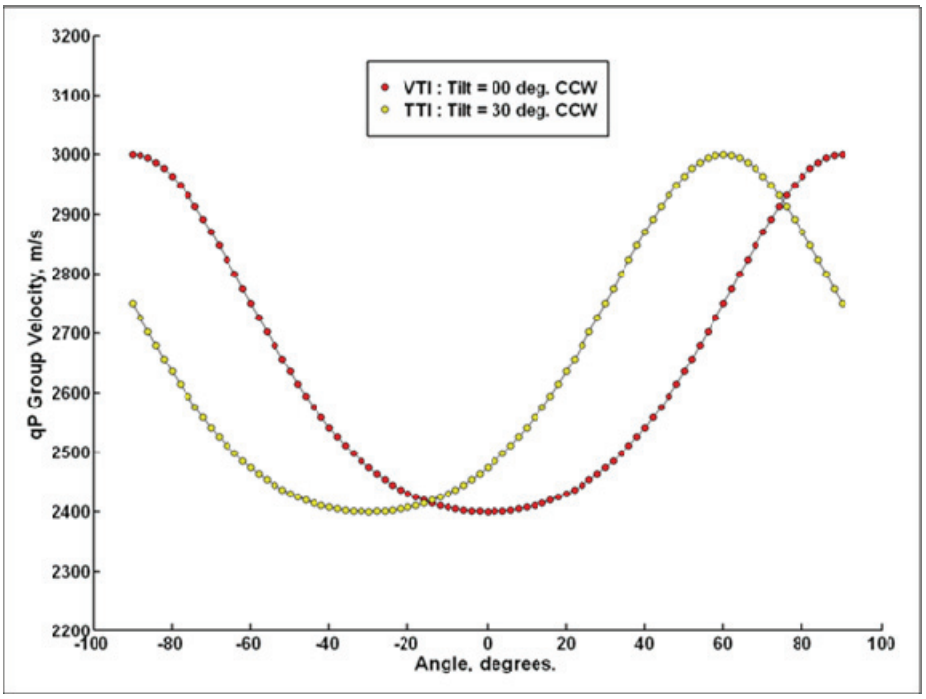

FIG. 1. qP group velocity $V_p(\emptyset)$ based on Equation 6, with V_h =3000 m/s, V_v =2400 m/s, and V_{45} = 2585 m/s. Red dots are VTI velocities; yellow dots are TTI velocities.

Figure 1 displays examples of group velocity $V_p(\emptyset)$ based on the Byun/Kumar formulation for traverse anisotropy. VTI occurs if the tilt angle φ equals 0°, and TTI results when the tilt angle φ is set to 30°.

Figure 2 shows rays and arrival times for a subsurface source and a set of subsurface receivers through a homogeneous medium. Raypaths are shown as blue lines. Arrival times for the isotropic case with velocity of 3000 m/s are compared with those for VTI anisotropy (φ = 0°), and for TTI anisotropy (φ = ±30°). The V_h, V_v, and V_{45} parameters are those for Figure 1. The TTI minimum arrival times are shifted up and down from the horizontal raypath position due to the change in the orientation of the maximum velocity

(V_h) axis. This behavior needs to be account for when analyzing and interpreting seismic arrival time moveouts, as is done, for example, in NMO analysis, in crosswell velocity tomography, and in microseismic hypocenter location.

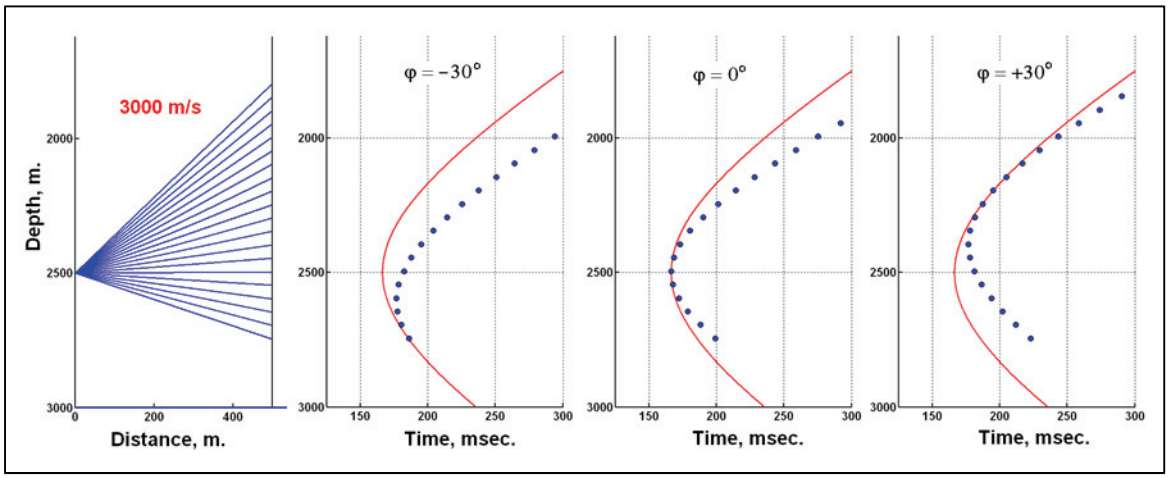

FIG. 2. Comparison of arrival times for homogeneous isotropic and TI media. The red curve shows arrival times for the isotropic case. The blue dots are arrival times with tilt angles of -30°, 0°, and +30° for the axis of symmetry of the TI anisotropy.

TWO-POINT RAY TRACING IN LAYERED VELOCITY MEDIA

Um and Thurber (1987) reported a raypath perturbation technique for two-point ray tracing through 2D heterogeneous velocity fields. I consider a similar ray-bending technique designed to be used for horizontally-layered media, in which any of the layers may exhibit TTI velocity anisotropy.

Figure 3 shows the case of two horizontal boundaries between three zones with different velocities. We wish to determine the travel path taken by a seismic signal in going from the source S through the interface to the receiver R. The source has coordinates $(x_s,\ z_s)$, while the receiver has coordinates $(x_r,\ z_r)$. The intersection point at the each of the interfaces has coordinates $(x_i,\ z_i)$.

The path has straight line segments in each of constant velocity zones, but will be bent at the interfaces. The bending occurs in such a way that the total path must conform to Fermat's principle, which states that the path must be one of least time. Two-point ray tracing reduces to determining the coordinates $(x_i,\ z_i)$ of the intersection points, given that the path must be one of least time.

$$\cos(\emptyset) = \Delta z/\sqrt{(\Delta x^2 + \Delta z^2)}\ , \tag{7}$$

$$\sin(\emptyset) = \Delta x/\sqrt{(\Delta x^2 + \Delta z^{2)}}\ . \tag{8}$$

Equations 7 and 8 express $\cos(\emptyset)$ and $\sin(\emptyset)$ in terms of the lengths of the straight-line ray segment between boundaries. Using them, Equation 5 is then cast in a form convenient for ray tracing through horizontal layers, with or without velocity anisotropy.

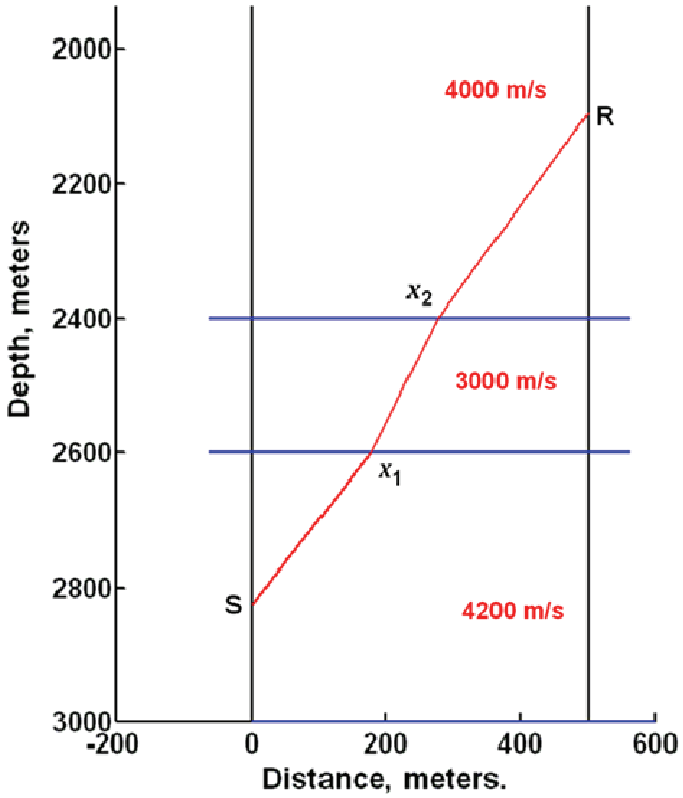

FIG. 3. Schematic of two-point ray tracing in layered media between a subsurface source S and a subsurface receiver R. All the layers have isotropic velocities except for the layer between 2400 m and 2600 m. This low velocity zone represents an anisotropic shale layer with VTI parameters of V_h =3000 m/s, V_v =2400 m/s, and V_{45} = 2585 m/s.

The length of the line segment between the source S and the intersection point 1 is

$$l_1 = \sqrt{(x_1 - x_s)^2 + (z_1 - z_s)^2}\ . \tag{9}$$

The length of the line segment between intersection points 1 and 2 is

$$l_2 = \sqrt{(x_2 - x_1)^2 + (z_2 - z_1)^2}\ . \tag{10}$$

The length of the line segment between the receiver R and point 2 is

$$l_3 = \sqrt{(x_r - x_2)^2 + (z_r - z_2)^2}\ . \tag{11}$$

The total travel time is

$$t = u_1 l_1 + u_2 l_2 + u_3 l_3\ . \tag{12}$$

where v_i and $u_i = 1/v_i$ are the seismic velocities and slownesses, respectively.

The source coordinates $(x_s,\ z_s)$ and the receiver coordinates $(x_r,\ z_r)$ are fixed. The depths z_1 and z_2 of the interfaces are also fixed. The only variables are the horizontal

coordinates x_1 and x_2 of the intersection points. If the path has minimum time, then the derivative of t with respect to x_1 and x_2 must be zero, i.e.:

$$u_1(x_1 - x_s)/l_1 - u_2(x_2 - x_1)/l_2 = 0 , \quad (13a)$$

$$u_2(x_2 - x_1)/l_2 - u_3(x_r - x_2)/l_3 = 0 , \quad (13b)$$

Since

$$(x_1 - x_s)/l_1 = \sin \emptyset_1 , \quad (x_2 - x_1)/l_2 = \sin \emptyset_2 , \quad (14)$$

$$(x_r - x_2)/l_3 = \sin \emptyset_3 ,$$

where $\emptyset_1$, $\emptyset_2$, and $\emptyset_3$ are incident and refracted angles, we have

$$u_1 \sin \emptyset_1 = u_2 \sin \emptyset_2 = u_3 \sin \emptyset_3 . \quad (15)$$

This is Snell's law stating that the horizontal component of slowness (the ray parameter) is continuous across the interfaces. Equations 14 and 12 show the equivalence of Fermat's principle and Snell's law.

In order to find the minimum time path, I must determine the intersection coordinates x_1 and x_2. This can be done either by using nonlinear optimization directly on Equation 12 to minimize t, or by employing a Newton-Raphson procedure to solve the system of nonlinear Equations 13a and 13b. Taking the first approach, I apply an iterative direct-search scheme similar to the pattern search algorithms described by Kolda et al. (2003) to find x_1 and x_2. The search begins with a set of starting values obtained by drawing a straight line between the source S and receiver R (see Figure 3).

Equation 12 can be expanded to include multiple layers. If source and receiver cross *n* boundaries, the total travel time would be the sum of (*n*+1) terms of the form $u_i l_i$:

$$t = u_1 l_1 + u_2 l_2 + u_3 l_3 \ ... + u_{n+1} l_{n+1} . \quad (16)$$

Moreover, TTI anisotropy can be included into one or more of the layers by defining u_i with equations 1 to 8 using appropriate values for the tilt angle φ and the velocities V_v, V_h, and V_{45}. Again, I find the Fermat raypath by using a direct search method to locate the intersection coordinates (x_i, z_i) that minimize the travel time t. Two checks may be used to ensure that the solutions x_i correspond to the minimum travel time:

1. At an intersection point x_i, the slowness $u_i(x_{i+1} - x_i)/l_i$ parallel to the interface must be equal on both sides of the layer boundary.
2. The first derivatives (determined numerically) of t with respect to each x_i must be zero or very close to zero.

RESULTS

The alternative to a two-point ray bending method for tracing a ray from a given source location to a given receiver location is the shooting method. The shooting method involves launching a ray at a particular take-off angle. As it encounters each boundary, the ray changes direction in order to maintain continuity of the ray parameter and conform to Snell's Law. The ray stops at a prescribed boundary (a borehole or the surface of the earth), and the end points may be far from a desired receiver position.

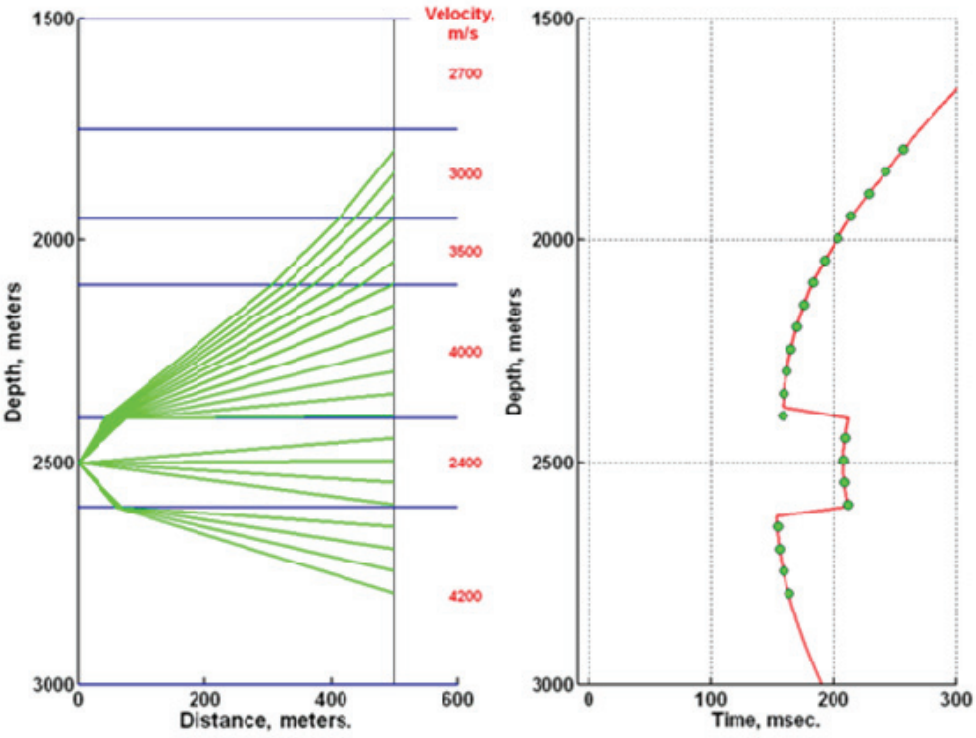

FIG 4. Left: rays traced from a source and 20 receivers embedded in a layered isotropic velocity model. Right: comparison of travel times from two-point ray tracing (green points) with those from shooting (red curve).

In order to obtain a travel path and time for a desired receiver, rays with different launch angles must be initiated so that their end positions span the desired receiver locations. Travel times at the desired receivers are then obtained by interpolation. Accurate interpolation of travel times through complex heterogeneous media may require many different rays to be launch. Thus, the shooting technique is inefficient when data for only a few receivers are needed, and interpolation errors may occur in shadow zones where the launched ray end points are sparse.

Figure 4 compares the arrival times though a layered medium determined by the shooting method with those produced by two-point ray bending. In this isotropic model, the travel times produced by both methods are identical. Figure 5 displays the travel paths and arrival times for the same velocity layers, but with the low-velocity zone beneath 2400 m now made anisotropic. The VTI parameters are the same as those for Figure 3: V_h =3000 m/s, V_v =2400 m/s, and V_{45} = 2585 m/s. This layer represents shale,

and its velocity of 2400 m/s is the vertical velocity that would be measured by a well-logging tool.

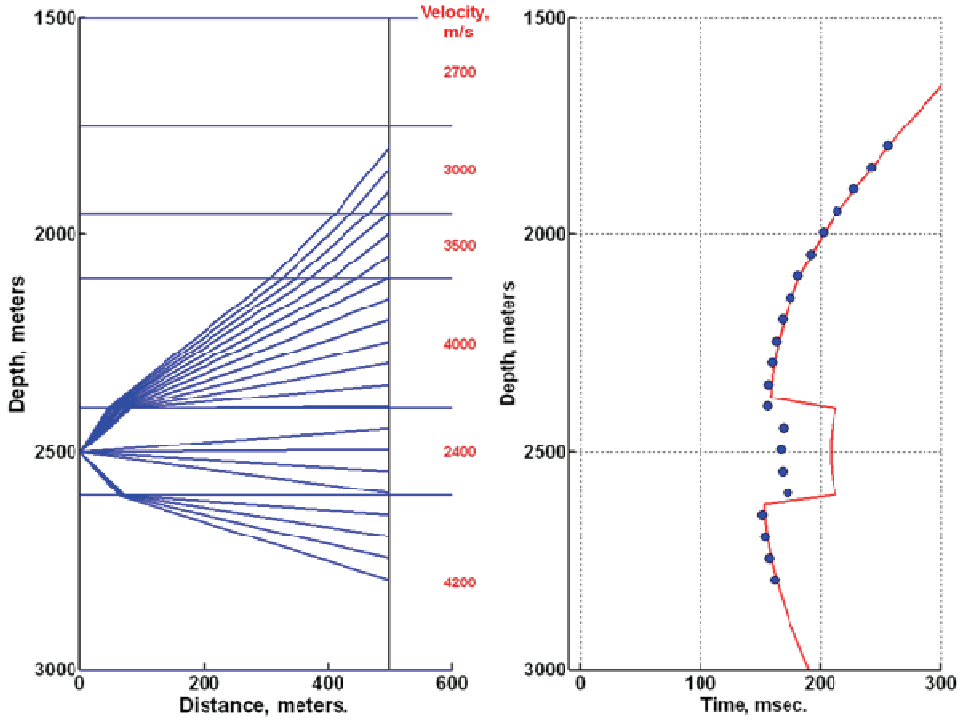

FIG. 5. Raypaths and arrival times for a source in the shale VTI velocity layer. Arrival times for the isotropic model with the shale velocity of 2400 m/s are plotted as the red curve. Blue dots are the arrival times for the layer being VTI with V_h =3000 m/s, V_v =2400 m/s, and V_{45} = 2585 m/s.

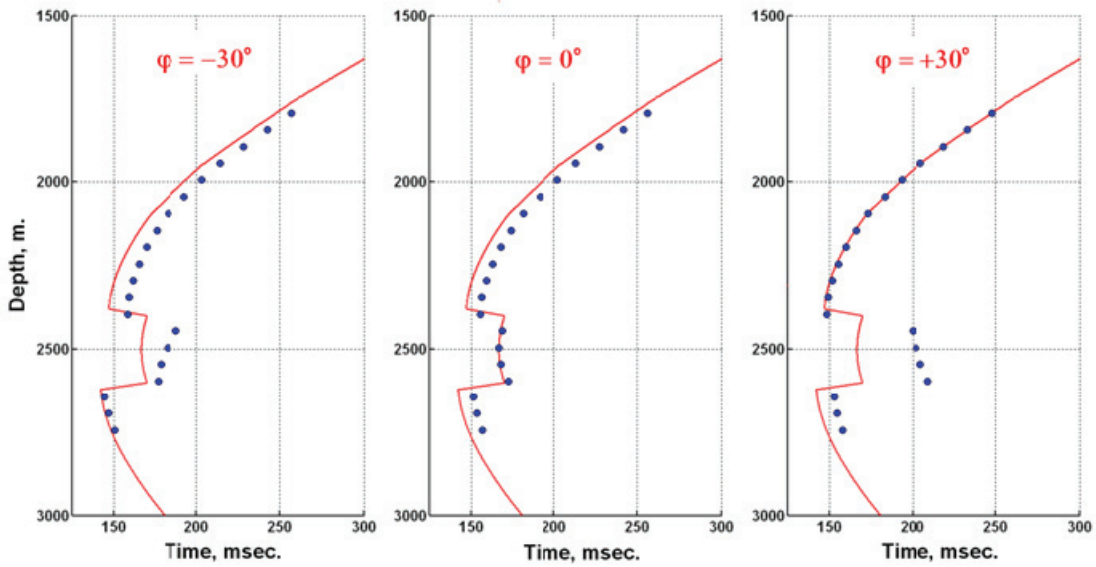

FIG. 6. Arrival times for transverse anisotropy in the shale layer for different tilt angles of the symmetry axis with V_h =3000 m/s, V_v =2400 m/s, and V_{45} = 2585 m/s. The red curve represents the isotropic model for which the isotropic shale velocity is 3000 m/s.

In the shale layer, the blue dots show earlier VTI arrival times compared to the red curve showing isotropic arrival times. This is because the raypaths within the shale layer are horizontal or nearly horizontal, and the VTI velocities associated with them are near the V_h value of 3000 m/s.

Figure 6 compares the arrival times for the VTI case and two TTI cases with the VTI symmetry axis in the shale tilted by ±30°. The arrival times for the tilted cases differ significantly from each other and from the VTI and isotropic cases. The figure suggests that that microseismic hypocenter location based on first arrival times may result in significant errors in the estimated position of a fracture event if TTI anisotropy is not taken into account.

SUMMARY AND DISCUSSION

1. The TTI discussed in the remarks above is restricted to tilt angles within the x-z plane. TTI associated with tilt angles out of this plane involves more complicated equations, but the problem is still tractable.

2. Because there is no need to calculate and invert Jacobian matrices repeatedly, direct search optimization rather than gradient–based inversion methods to locate the intersections (x_i, z_i) results in a faster and more efficient procedure.

3. Compared to the shooting method, where interpolation between receiver positions is necessary, two-point ray tracing deals with different source-receiver configurations much more efficiently. Such ease and flexibility allow us to quickly produce the raypaths and arrival times for downhole receiver arrays needed for analyzing VSP, crosswell, and microseismic monitoring data.

4. Although this report addresses ray tracing through horizontal boundaries only, the method can easily include sloping straight boundaries. It may even be possible to deal with gently curving boundaries. In principle, the method also can be extended to include out-of-plane raypaths, resulting in 3D two-point ray tracing through anisotropic layered media.

ACKNOWLEDGEMENTS

This research has been supported by NSERC and the industrial sponsors of CREWES.

REFERENCES

Byun, B.S., Corrigan, D., and Gaider, J.E., 1989. Anisotropic velocity analysis for lithology discrimination, Geophysics, **54**, 1566-1574.

Casasanta, L., Drufucca, G., Di Milano, P., Andreoletti, C., and Panizzardi, J., 2008. 3D anisotropic ray tracing by raypath optimization, Expanded Abstr., SEG 78th Ann. Int. Mtg.

Kolda, T.G., Lewis, R.M., and Torczon, V., 2003. Optimization by direct search: new perspectives on some classical and modern methods, Soc. Indus. And Appl. Math., **45**, 385-422.

Kumar, D., Sen, M.K., and Ferguson, R.J., 2004. Traveltime calculation and prestack depth migration in tilted transversely isotropic media, Geophysics, **69**, 37-44.

Thomsen, L., 1986. Weak elastic anisotropy, Geophysics, **51**, 1954-1966.

Um, J., and Thurber, C., 1987. A fast algorithm for two-point ray tracing, Bulletin of the Seismological Soc. Am., **77**, 972-986.